Exploring Slow Feature Analysis for Extracting Generative Latent Factors

Max Menne[a], Merlin Schüler[b] and Laurenz Wiskott[c]

Institute for Neural Computation, Ruhr University Bochum, Universitätsstraße 150, 44801 Bochum, Germany

Keywords: Slow Feature Analysis, Representation Learning, Generative Models.

Abstract: In this work, we explore generative models based on temporally coherent representations. For this, we incorporate Slow Feature Analysis (SFA) into the encoder of a typical autoencoder architecture. We show that the latent factors extracted by SFA, while allowing for meaningful reconstruction, also result in a well-structured, continuous and complete latent space – favorable properties for generative tasks. To complete the generative model for single samples, we demonstrate the construction of suitable prior distributions based on inherent characteristics of slow features. The efficacy of this method is illustrated on a variant of the Moving MNIST dataset with increased number of generation parameters. By the use of a forecasting model in latent space, we find that the learned representations are also suitable for the generation of image sequences.

1 INTRODUCTION

Recently, deep generative models have yielded impressive results in the artificial generation of realistic high-dimensional image (Karras et al., 2018; Kingma et al., 2016; Van den Oord et al., 2016b), audio (Van den Oord et al., 2016a; Mehri et al., 2016) and video (Denton and Fergus, 2018; Tulyakov et al., 2018) data. At the same time, unsupervised representation learning has been known to aid effective learning in goal-oriented frameworks such as reinforcement learning (Sutton and Barto, 2018) or supervised learning (Goodfellow et al., 2016) when rewards or labels are sparse. While the use of generative factors as effective representations in goal-directed learning is a strong focus of current research (Yarats et al., 2019; Hafner et al., 2020), the back-direction less so.

To enable unsupervised training of generative models usually a maximum-likelihood criterion and the reconstruction error are used in combination as an optimization objective (Kingma and Welling, 2019). The majority of realizations of generative models for complex and high-dimensional data are based either on the Variational Autoencoder (VAE) (Kingma and Welling, 2013) or Generative Adversarial Networks (GANs) (Goodfellow et al., 2014).

We explore a new class of generative models that is optimized using the principle of temporal coherence in combination with the reconstruction error. The latter is realized by using an autoencoder architecture and reconstruction loss, while the former is realized by Slow Feature Analysis (SFA). In contrast to the strict end-to-end training procedure of VAEs and GANs, this allows for principle-based extraction and subsequent processing of latent factors for generative purposes, offering separated and more detailed analyses. SFA uses the principle of slowness as a proxy for the extraction of low-dimensional descriptive representation from, possibly high-dimensional, time-series data or data for which other pairwise similarities can be defined. In our models, these obtained low-dimensional representations are considered as latent factors, since they often encode the elementary properties of the data-generation process (Franzius et al., 2007; Franzius et al., 2011; Schüler et al., 2019). First theoretical considerations for modelling slow features as generative latent factors have already been introduced in (Turner and Sahani, 2007), but are restricted to the linear case. In contrast, our models are based on non-linear PowerSFA (Schüler et al., 2019). Its applicability to any differentiable encoder/decoder allows for significantly more powerful encoding and efficient processing of complex and possibly high-dimensional data, while it can be trained end-to-end with respect to different objective functions.

[a] https://orcid.org/0000-0002-0808-497X
[b] https://orcid.org/0000-0002-9809-541X
[c] https://orcid.org/0000-0001-6237-740X

Menne, M., Schüler, M. and Wiskott, L.
Exploring Slow Feature Analysis for Extracting Generative Latent Factors.
DOI: 10.5220/0010391401200131
In *Proceedings of the 10th International Conference on Pattern Recognition Applications and Methods (ICPRAM 2021)*, pages 120-131
ISBN: 978-989-758-486-2

We start by introducing SFA in Section 2. The experiments presented in Section 3 are based on different models and datasets, consisting of synthetic image sequences, described in Section 3.1 and 3.2. Our analyses focus, in particular, on the latent factors. We investigate the relationship between their slowness and reconstructability in Section 3.3 as well as the structure and properties of the resulting latent space for generative purposes in Section 3.4. Based on these findings, we propose a method for the construction of a prior distribution over the latent factors in Section 3.5. We show that samples from this prior distribution are suitable for the generation of new images using the aforementioned decoder. Finally, we extend one of our models by a forward predictor over the extracted representation and demonstrate the generation of image sequences. In Section 4, we discuss our results and give future directions.

2 SLOW FEATURE ANALYSIS

SFA is an unsupervised learning algorithm which utilizes the principle of slowness to extract low-dimensional data-generating factors. The principle of slowness states that high-dimensional data streams, which change rapidly over time, are generated by a small number of comparatively slowly varying factors.

SFA therefore solves the optimization problem of the extraction of slow, meaningful features: Given a time series $\{\mathbf{x}_t\}_{t=0,1,\ldots,N-1}$ consisting of data points $\mathbf{x}_t \in \mathbb{R}^d$, find a continuous input-output function $g: \mathbb{R}^d \to \mathbb{R}^e$ so that

$$\min_g \quad \langle \|g(\mathbf{x}_{t+1}) - g(\mathbf{x}_t)\|^2 \rangle_t \tag{1a}$$

$$\text{s.t.} \quad \langle g(\mathbf{x}_t) \rangle_t = \mathbf{0}, \tag{1b}$$

$$\langle g(\mathbf{x}_t) g(\mathbf{x}_t)^T \rangle_t = \mathbf{I}_e. \tag{1c}$$

In this context the time average is denoted by $\langle \cdot \rangle_t$ and $\mathbf{I}_e$ refers to the e-dimensional unit matrix. To ensure an ordering from the slowest to the fastest varying feature, the following constraint can be additionally applied for $i < j$:

$$\begin{aligned}\Delta(g_i) &= \langle \|g_i(\mathbf{x}_{t+1}) - g_i(\mathbf{x}_t)\|^2 \rangle_t \\ &\leq \langle \|g_j(\mathbf{x}_{t+1}) - g_j(\mathbf{x}_t)\|^2 \rangle_t = \Delta(g_j).\end{aligned} \tag{2}$$

These constraints ensure unique (zero mean, equation (1b)), non-trivial and informative (unit variance and decorrelation, equation (1c)) solutions.

In the past several different variants (Böhmer et al., 2011; Franzius et al., 2007; Escalante-B and Wiskott, 2020) of the original SFA algorithm (Wiskott and Sejnowski, 2002) have been proposed to overcome limitations and improve the performance of SFA.

A recently introduced version of the SFA algorithm is the so-called Power Slow Feature Analysis (PowerSFA) (Schüler et al., 2019), which is based on differentiable approximated whitening. This allows the combination of the SFA optimization problem with differentiable architectures, such as neural networks, and the optimization in form of a gradient-based end-to-end training procedure.

One of the main steps in the SFA algorithm is the whitening of the data which is essential to fulfill the SFA constraints (equations (1b) and (1c)). The central idea of PowerSFA consists of whitening the data within a differentiable whitening layer. This whitening layer can be applied to any differentiable architecture that is used as a function approximator and ensures that the outputs met the SFA constraints.

Mathematically, PowerSFA can be formalized as follows: Given a dataset $\mathbf{X} = [\mathbf{x}_0, \mathbf{x}_1, \ldots, \mathbf{x}_{N-1}] \in \mathbb{R}^{d \times N}$ the output $\mathbf{Y} \in \mathbb{R}^{e \times N}$, which approximately matches the SFA constraints, is calculated by

$$\mathbf{Y} = \mathcal{W}(\mathbf{H}) \quad \text{with} \quad \mathbf{H} = \tilde{g}_{\boldsymbol{\theta}}(\mathbf{X}).$$

The approximated whitening by means of the whitening layer is described by $\mathcal{W}: \mathbb{R}^{N \times e} \to \mathbb{R}^{N \times e}$ and a differentiable function approximator, like a neural network, parameterized by $\boldsymbol{\theta}$ with $\tilde{g}_{\boldsymbol{\theta}}: \mathbb{R}^d \to \mathbb{R}^e$. For optimization with respect to the slowness principle, an error measurement based on a general differentiable loss function such as

$$\mathcal{L}(\mathcal{S}, \mathbf{Y}) = \frac{1}{N} \sum_i \sum_j s_{ij} \|\mathbf{y}_i - \mathbf{y}_j\|^2 \tag{3}$$

can be used. In this case s_{ij} describes the similarity between two data points $\mathbf{x}_i$ and $\mathbf{x}_j$.

3 EXPERIMENTS

In this paper, we focus on the question if generative latent factors can be extracted using SFA. The central approach for the development and analysis of a generative model is based on the embedding of SFA into the structure of an autoencoder. From this idea, we derive two main models, which build – in combination with different datasets based on image sequences – the foundation for the experiments. The analyses are divided into the following three key aspects:

Reconstructability. We analyze the reconstructability of the input data based on the extracted features and investigate how the SFA constraints influence the reconstructions.

Structure of the Latent Space. We explore if the latent space defined by the extracted latent factors is structured in a continuous and organized manner, which is therefore suitable for generative purposes. Further, the complexity and possible dependencies between individual factors are considered.

Prior Distribution Over Latent Factors. We try to manually construct meaningful underlying prior distributions and check whether samples of these distributions can be decoded in a meaningful way to generate new data.

3.1 Models

We start by introducing the central models, which share the same general architecture consisting of a neural encoder and decoder network. All models are trained with the ADAM optimization algorithm (Kingma and Ba, 2014) with Nesterov-accelerated momentum (Dozat, 2015).

3.1.1 Encoder-Decoder Model

The Encoder-Decoder model consists of an encoder and decoder network. The encoder is a simple neural network followed by the PowerWhitening layer of the PowerSFA framework and embeds the input data into the latent space. The input layer of the encoder takes a single 64×64 pixel greyscale image. After flattening, the resulting 4096-dimensional vector is reduced to the dimensionality of the latent space by a dense layer. The output of the dense layer is finally whitened by the subsequent PowerWhitening layer, which simultaneously represents the output layer of the encoder and outputs the latent factors. The decoder network consists of a fully-connected feedforward neural network. The decoder receives the latent factors as input and processes them by a block of five dense layers. These layers consist of 64, 128, 256, 512 and 4096 units and therefore upsample the activations back to a 4096-dimensional vector or respectively after reshaping to a 64×64 pixel greyscale output image. The units in the first four dense layers are implemented by Rectified Linear Units (ReLUs), while for the activation of the units in the fifth layer a Sigmoid activation function is used. A visualization of the encoder and decoder network is provided in Appendix A.

The training procedure of the Encoder-Decoder model is divided into two steps. First, we train the encoder with respect to the general slowness objective of the PowerSFA framework, introduced in equation (3) and denoted in the following as $\mathcal{L}_{\text{SFA}}(\mathcal{S},\mathbf{Y})$. In a second phase the decoder network is optimized with respect to the cross-entropy loss $\mathcal{L}_{\text{CE}}(\mathbf{X},\tilde{\mathbf{X}})$ between the original input images $\mathbf{X}$ and the computed output images $\tilde{\mathbf{X}}$.

Due to the division of the training process, the decoder does not influence the encoder and an unimpaired learning of a function for the extraction of slowly varying features by the encoder is guaranteed.

3.1.2 Slowness-Regularized Autoencoder Model

The Slowness-Regularized Autoencoder (SRAE) model is very similar to the Encoder-Decoder model, but has the difference that the encoder and decoder are combined into an autoencoder. We omit the input layer of the decoder and append the remaining layers directly to the former output layer of the encoder.

The SRAE model is optimized in an end-to-end fashion with respect to a composite loss function. It consists of the sum of the previously introduced cross-entropy loss $\mathcal{L}_{\text{CE}}(\mathbf{X},\tilde{\mathbf{X}})$ and the general slowness objective $\mathcal{L}_{\text{SFA}}(\mathcal{S},\mathbf{Y})$, which is additionally weighted by a weighting factor α:

$$\mathcal{L}_{\text{SRAE}}(\mathbf{X},\tilde{\mathbf{X}},\mathcal{S},\mathbf{Y}) = \mathcal{L}_{\text{CE}}(\mathbf{X},\tilde{\mathbf{X}}) + \alpha \cdot \mathcal{L}_{\text{SFA}}(\mathcal{S},\mathbf{Y}) \quad (4)$$

The calculated error is back-propagated through the entire architecture. The reconstruction error affects thus not only the decoder and its parameters but also the encoder, its parameters and consequently the encoding.

By choosing the hyperparameter $\alpha = 0$, the SRAE model represents an autoencoder with whitened latent variables, but without regularization within the loss function. We use this specific configuration as a baseline. In contrast, for large values of α, a link to the previously introduced Encoder-Decoder model is established in the limiting case, as the reconstruction objective has almost no influence in relation to the slowness objective anymore.

3.2 Datasets

We evaluate our models on synthetic image data with different generating attributes. Using affine transformations like translation, rotation or scaling, image sequences with images of the dimension 64×64 are generated from single 28×28 pixel images of the MNIST (LeCun et al., 2010) dataset. This dataset generation therefore combines the transformations used in the affNIST dataset (Tieleman, 2013) with the idea to generate not only single images but image sequences as in the Moving MNIST (MMNIST) (Srivastava et al., 2015) dataset. This results in an extended version of the MMNIST dataset with additional possible transformations besides the translation of a digit.

The datasets can be divided into two classes. The first class is formed by the so-called moving sequences with the defining property of variation in position. In this case, an image sequence is build by moving a single digit in the 64×64 frame on linear trajectories which are reflected at the edges. As an alternative to the variation of the identity of the used digit, further, a rotation or scaling of the digit can be applied in conjunction with the variation in position. The second class is based on so-called static sequences in which the position of the digit is fixed in the center of the 64×64 pixel image. For this class of datasets, we vary the identity and rotation or scaling of the digit.

Besides the image sequences, each dataset is augmented by a similarity matrix $\mathcal{S}$, which defines the similarity between all images. To extract slowly varying features, the similarity is based on the temporal proximity, which can be expressed by the Kronecker delta $s_{ij} = \delta_{i,j+1}$ leading to a connection between consecutive images. Alternatively, the similarity matrix can define a more general neighborhood-based relationship based on certain attributes of the individual images like position or identity of the digit. This allows an optimization with respect to a graph-based embedding.

This dataset generation enables the construction of arbitrarily large and complex datasets as well as a precise control over the data-generating attributes. These properties facilitate the exploration and analysis of the extracted latent factors.

3.3 Slowness versus Reconstructability

In this section, we investigate the relationship between the principle of slowness and the reconstructability based on the extracted latent features. The experiment examines whether these two principles work in contradiction to each other and whether reconstructions from the latent features are considerably more difficult due to their slowness.

For this purpose, we compare the Encoder-Decoder model and the SRAE model. Within the composite loss function of the SRAE model (equation (4)), we weight the SFA loss by a factor of $\alpha = 15$. Additionally, an autoencoder with whitened latent factors corresponding to the SRAE model with a weighting factor $\alpha = 0$ is used as a baseline. We train the models over 1000 epochs on a dataset with variation in position and identity, where the identity is chosen from a set of three different digits. The position changes on linear trajectories within the image sequences, which consist of five images each. From image sequence to image sequence the identity is varied. In total, we use 8000 connected sequences and a similarity matrix based on temporal coherence. The dimensionality of the latent space is set to five in all models.

The resulting learning curves with respect to the reconstruction error are plotted in Figure 1a. The smallest reconstruction error is achieved by the autoencoder with whitened latent factors, followed by the SRAE model with a weighting factor of $\alpha = 15$ and the Encoder-Decoder model. From a global perspective, all three models show qualitatively similar monotonically falling learning curves with clear convergence behavior. The autoencoder with whitened latent variables converges fastest, while the Encoder-Decoder model converges most slowly.

These results show that the quality of the reconstructions is inhibited and reduced by restricting the latent factors to slowly varying features, however, these effects can be considered to be within an acceptable range, as the reconstruction errors and the direct comparison of reconstruction examples of the models given in Figure 1b demonstrate.

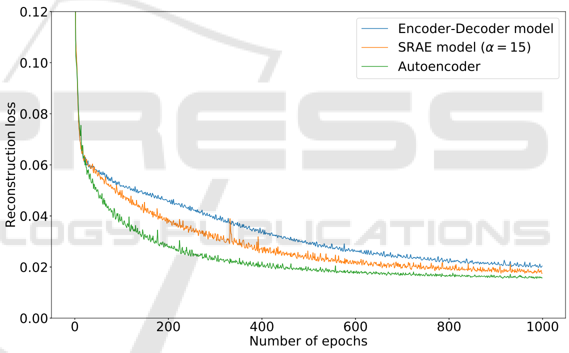

(a)

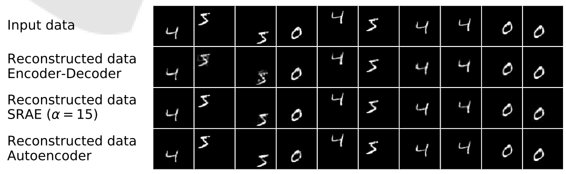

(b)

Figure 1: Progression of the reconstruction error (a) and reconstructions (b) of the Encoder-Decoder model, the SRAE model with weighting factor $\alpha = 15$ and an autoencoder with whitened latent variables on a dataset with variation in position and identity.

The results of this experiment further indicate that the SRAE model with different weighting factors α enables an interpolation between an autoencoder and the Encoder-Decoder model. In an additional analysis, provided in Appendix B, we trained and compared several SRAE models with different weighting factors α and could show that this is indeed the case. As the weighting of the SFA loss within the composite loss of the SRAE model increases, the SFA loss decreases while the reconstruction loss increases. Based on this analysis, we further deduce that a weighting factor of $\alpha = 15$ offers a good compromise between a small reconstruction error and the extraction of slowly varying latent factors.

3.4 Latent Factors and Reconstructions

In this section, we analyze the extracted latent factors and the structure of the latent space, in particular, with regard to its continuity, completeness and complexity introduced by dependencies between the individual latent factors. By the term continuity, we denote the property that two close points in the latent space result in two similar reconstructions, while the term completeness refers to the existence of a meaningful reconstruction for each point in the latent space.

3.4.1 Explorations on Static Sequences

At first, embeddings and reconstructions of static sequences are considered. As an initial investigation of the continuity and completeness of the latent space, we perform a latent space exploration on four different models. We use the Encoder-Decoder model and the SRAE model with weighting factor $\alpha = 15$. In addition, two autoencoders, one with and one without whitening of the latent variables, are trained. These autoencoders therefore correspond to the SRAE model with or respectively without the PowerWhitening layer and a weighting factor of $\alpha = 0$. In all models the latent space has two dimensions.

The dataset for this experiment includes only a variation in identity. To generate the dataset, we use five variations of each of the ascending identities from `0` to `9` in succession. The similarity matrix encodes successive images as similar and connects the identities `0` and `9`. The identity is therefore in this case a cyclic variable, which can be encoded by two latent factors. SFA is well-known to extract these factors when they are clearly reflected in sample similarity.

The latent spaces of the trained models are traversed in 200 equally large steps in both dimensions. For each latent sample, we compare the reconstruction with the input images by calculating the cross-entropy and assign the most appropriate identity. The color-coding of the samples represents this assignment, while the saturation further indicates how closely the reconstruction matches the assigned input image. A high saturation indicates a high degree of correspondence. Figure 2 shows the resulting feature maps of the four different models.

By comparing the visualizations of the latent space of the autoencoders (Figure 2a and 2b), it is evident that the whitening of the latent factors by means of the PowerWhitening layer leads to a significantly more compact structure of the latent space. This directly transfers to a higher degree of completeness and is also reflected in the reconstruction error on the training data. Besides the fact that the reconstruction errors of the autoencoders are overall slightly lower than those of the models with inclusion of the SFA objective, it is interesting that the autoencoder including the PowerWhitening layer achieves a lower reconstruction error (0.0127) than the autoencoder without whitening of the latent factors (0.0156).

Considering the continuity, the local changes of saturation within and between clusters of different identities indicate that the identities merge smoothly and that also continuous transitions between the individual variations of an identity exit.

The SFA objective further clearly structures the latent space and arranges the embeddings of the ascending identities in clockwise order in circular sectors as the visualizations of the latent space of the SRAE model (Figure 2c) and Encoder-Decoder model (Figure 2d) show.

We therefore conclude that the SFA objective and the associated constraints, implemented in the SRAE and Encoder-Decoder model, enable a well-structured, continuous and complete latent space in the case of data with variation in identity. Experiments on equivalent datasets with variation in rotation or scaling show qualitatively similar results and support these statements.

In a further experiment, we analyze more complex datasets with two varying attributes and focus on the disentanglement of the latent factors as well as the resulting complexity of the latent space. We generate two datasets with variation in rotation (cyclic) in steps of ten degrees and additionally six different scales (acyclic) or ten different identities (acyclic). The similarity matrices to these datasets define a neighborhood-based relationship. Images with successive rotation, scaling or identity attributes are therefore encoded as similar. On these two datasets, we train the SRAE model with three latent factors.

Figure 3 shows the embeddings of the two considered datasets. In both embeddings the rotation is encoded in the first two dimensions, while the scaling or respectively the identity is embedded in the third dimension.

For the data with variation in rotation and scaling, the latent factors are strongly disentangled and only a slight proportional dependence between the radii of the cyclic embedding of the rotation and the scaling

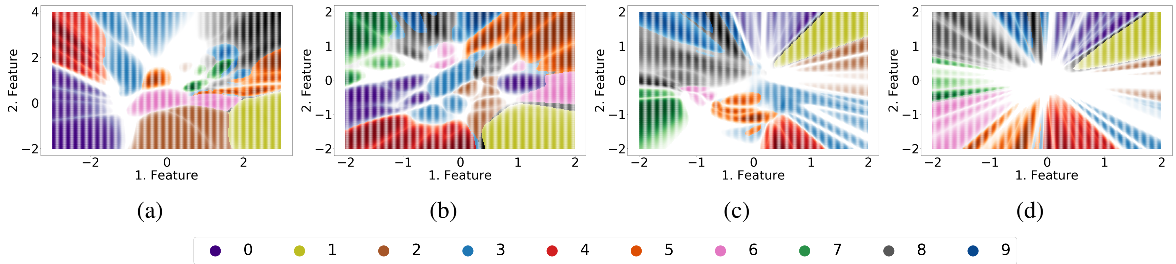

Figure 2: Visualization of the latent space of the autoencoder (a), autoencoder with PowerWhitening layer (b), SRAE model ($\alpha = 15$) (c) and Encoder-Decoder model (d) trained on a dataset including ten different identities in five variations each. The color-coding of the individual samples represents the corresponding identity, while the saturation indicates the degree of correspondence.

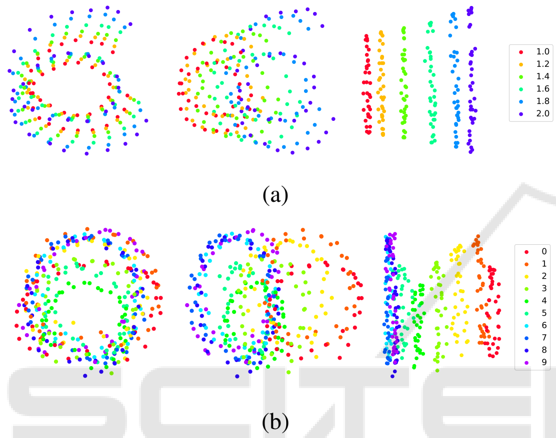

Figure 3: Three views of the embedding of the datasets with variation in rotation and scaling (a) and variation in rotation and identity (b).

is visible. The spiral shape of the generally circular structure of the embedding can be attributed to strong structural similarities among certain rotations of the used identity 4. We further note that the embedding computed in this example matches the embeddings and results of the coding of the NORB dataset with similar data-generating factors as computed and presented in (Schüler et al., 2019) qualitatively well. Based on the unique embedding of the training data, the decoder is also able to reconstruct the data accurately.

In the embedding of the data with variation in rotation and identity, the embeddings of some identities overlap and are thus not uniquely encoded with respect to the third dimension. Furthermore, the radii of the circular embedding of the rotation seem to depend more strongly on the respective identity. This ambiguity of the embedding is also reflected in poor reconstructions of the input data.

(Turner and Sahani, 2007) identify a possible weakness of the standard SFA formulation in that it confounds categorical and continuous latent factors during extraction, which might be a reason for the aforementioned ambiguity. We try to address this possible weakness by further development of the Encoder-Decoder model in Section 3.4.3.

3.4.2 Explorations on Moving Sequences

Analogous to the analyses on the static sequences, we also investigate the embeddings of the moving sequences. In addition to the variation of the position, the rotation or alternatively the identity is varied in this case. For this purpose the position is chosen from a grid structure consisting of 18×18 points, the orientation (cyclic) is changed in steps of 20 degrees and the identity (acyclic) is varied between 0 and 9. For both datasets, the neighborhood-based method is used to determine the similarity matrix. We have trained both the SRAE model as well as the Encoder-Decoder model on these two datasets. Since the results are almost identical, we discuss here only the embeddings and reconstructions of the SRAE model.

Figure 4 shows the embeddings of the two considered datasets in the three-dimensional latent space. The global structure of these embeddings has the form of a rectangular hyperbolic paraboloid. When projecting these embeddings onto the plane spanned by the first and third dimension, a grid-shaped coding of the 18×18 positions can be identified.

In the case of the dataset with variation in position and rotation, each node of the grid consists of a local structure, which encodes the rotation, as apparent from the color-coding. The individual embeddings within the local structure are arranged in a continuous manner with respect to the corresponding rotation and reflect the global structure by forming a hyperbolic paraboloid. These structures on both global and local scales blur towards the edges of the latent space.

In contrast, no clear local structure can be identified in the embedding of the dataset with variation in position and identity. The individual regions appear much more disorganized and we could not identify a principal structure of the embedding of the identities.

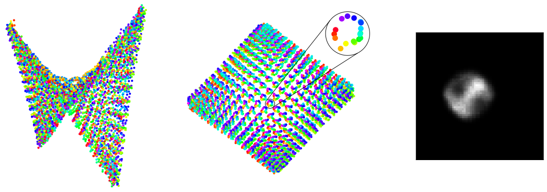

(a)

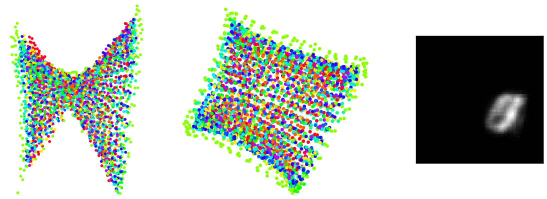

(b)

Figure 4: Front and top view of the embedding as well as a single exemplary reconstruction of the datasets with variation in position and rotation (a) and variation in position and identity (b).

Overall, the embeddings of the considered moving sequences form complex structures with strong dependencies between the latent factors. These hierarchical structures may be due to strongly differing levels of slowness of the data-generating factors. It is conceivable that the variation of the position compared to the variation of the rotation or identity results in features that are significantly slower and therefore easier to extract. Additionally, the combination of continuous and categorical attributes in the case of the dataset with variation in position and identity could also impede the formation of a local structure. Through further experiments with higher dimensional latent spaces, we could exclude the restriction to three dimensions as a reason for such embeddings. The exemplary reconstructions demonstrate that the position is precisely reconstructed, while the rotation or identity can hardly be recovered at all. The decoder is therefore not able to learn any exact mapping of the hierarchical encoding of the varying attributes to corresponding reconstructions.

3.4.3 Separated Extraction of Latent Factors

In this section, we introduce an approach for the separated extraction of continuous and categorical data-generating attributes. Neither the SFA optimization problem nor the associated algorithms provide or consider such a separation. The aim of this differentiation is to achieve a better structuring and stronger disentanglement of the latent factors as well as a better reconstructability.

This approach is motivated by the observations of the previous experiments on the static and moving sequences and is biologically plausible. Furthermore, a first theoretical approach along these lines has already been presented in (Turner and Sahani, 2007), which, in contrast to our approach, augments the set of continuous latent variables within a probabilistic SFA model by a set of binary variables and does not implement an explicitly separated extraction.

We implement this approach by extending the Encoder-Decoder model and analyze it in the context of moving sequences with variation in 36×36 positions and the identities from 0 to 9. In more general terms, the data is therefore composed of the categorical attribute of the object identity, which can also be described as the “What” information, and the continuous attribute of the object position, also referred to as the “Where” information.

The main idea is based on the separation of the extraction of the features by using two encoders. One of them is trained to extract continuous features whereas the other one is trained to extract categorical features. Applied to the dataset used here, this results in a What-Encoder, which extracts the identity in a single feature, and a Where-Encoder, which is responsible for encoding the position within two features. The extracted latent factors are then combined to define the latent space with corresponding continuous and categorical dimensions. Finally, the decoder reconstructs the data based on the samples of this combined latent space.

For the successful implementation of this model, the training of the encoders is of particular relevance. For both encoders, we use the identical image data but specific similarity matrices. To train the What-Encoder, all images with the same identity independent of their position are encoded as similar. The similarity matrix for the Where-Encoder encodes those images as similar which differ in their positioning only by a maximum of two pixels independent of the respective identity. The decoder is finally trained on the combined latent space and the corresponding input images.

Considering the embedding of the dataset plotted in Figure 5a, a simple and unique encoding of the data can be observed. The first two latent factors encode the position, whereas the identities are encoded by discrete values along the third dimension, as apparent from the color-coding. The latent factors are thus strongly disentangled and only a slight proportional dependence between the scale of the position coding and the third dimension is visible. Such dependencies can be easily addressed by constructing an adequate sampling model, as illustrated in Section 3.5.1. Figure 5b further demonstrates that the samples of the latent space can be meaningfully reconstructed by the decoder.

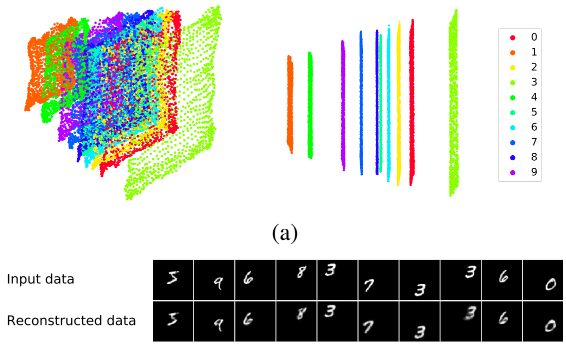

(a) (b)

Figure 5: Two different views of the combined embedding (a) of the dataset with variation in position and identity computed by the What- and Where-Encoder as well as exemplary reconstructions (b) computed on the basis of the latent samples by the decoder of the What-Where Encoder-Decoder model.

We conclude that this approach allows the generation of a simple and well-structured latent space whose samples can be reconstructed with high precision by the decoder. Especially in comparison to the results obtained in the last Section 3.4.2 using the SRAE model trained on a slightly simpler but nearly identical dataset, significant improvements in both encoding as well as decoding are achieved by using the What-Where Encoder-Decoder model.

These results therefore support the hypothesis that a separated extraction and segregated treatment of continuous and categorical variables is a reasonable approach to compute structural simple and disentangled embeddings. In the case of the moving sequences considered in this experiment, additionally, the otherwise dominant variation in position is extracted separately and thereby avoids inhibitions and deterioration of the extraction of other data-generating attributes.

This approach is, of course, not limited to the data-generating attributes considered in this example, but can also be generalized and applied to or extended by other varying attribute combinations. We assume that, in particular, the complexity of the latent space in terms of dependencies between the latent factors increases only moderately when adding further varying attributes, due to the disentanglement of these factors obtained by the separated extractions.

A limitation and prerequisite of this approach results from the additionally required information about the relations of the training images to compute the different similarity matrices used to train the individual encoders. However, it should be noted that even a partially separated extraction according to the available information might lead to significantly better results and therefore be useful.

3.5 Prior Distributions and Data Generation

For one of the main goals of generative models – the generation of new data – the prior distribution over the latent factors is a key element, since it determines in which way samples are drawn from the latent space and accordingly new data is generated. SFA in general and explicitly the models presented in this paper provide latent factors but no prior distribution over these factors, as no complete probabilistic model for (non-linear) SFA is known. In this section, we therefore present two approaches to generate new meaningful data on the basis of these extracted latent factors.

3.5.1 Definition of Prior Distributions over Latent Factors

Motivated by the results of Section 3.4, we define parameterized prior distributions, which are subsequently fit to the latent factors of a concrete dataset. These prior distributions are constructed based on characteristic structures identified in the previous sections. Specifically, different combinations of cyclic and acyclic variables result in distinct embeddings. One example for this is the elliptic conical frustum as the consequence of variations in rotation and scale. This is supported by structurally similar embeddings found in (Schüler et al., 2019). For sequences with variation in position and identity, the What-Where Encoder-Decoder model provides an embedding that can be well described by a rectangular frustum with multiple rectangular layers. Figure 6 visualizes these structures.

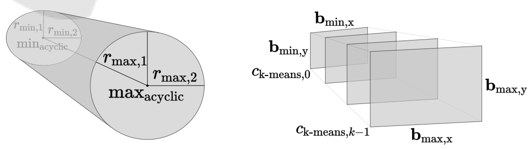

(a) (b)

Figure 6: Parameterized fundamental structures in form of a hollow conical frustum with elliptical bases (a) and a rectangular frustum consisting of multiple rectangular layers (b) used to define the prior distributions.

Points in both structures can be parameterized by a small set of parameters. For static sequences, we can build a prior distribution by assuming independent uniform distributions along the height of the frustum and the angle on the elliptical base. The parameter set therefore consists of the interval limits $[\min_{\text{acyclic}}, \max_{\text{acyclic}}]$ of the continuous uniform distribution along the height and the two pairs of radii

$\mathbf{r}_{\min}$ and $\mathbf{r}_{\max}$ of the elliptical bases. A sample $\mathbf{z} = (z_1, z_2, z_3)^T$ in latent space is then given by

$$z_1 = \cos(\phi) \cdot r_1, \quad (5a)$$

$$z_2 = \sin(\phi) \cdot r_2, \quad (5b)$$

$$z_3 \sim U(\min_{\text{acyclic}}, \max_{\text{acyclic}}) \quad (5c)$$

$$\text{with} \quad \phi \sim U(-\pi, \pi) \quad (5d)$$

$$\text{and} \quad (r_1, r_2)^T = h \cdot (\mathbf{r}_{\max} - \mathbf{r}_{\min}) + \mathbf{r}_{\min}, \quad (5e)$$

$$h = \frac{z_3 - \min_{\text{acyclic}}}{\max_{\text{acyclic}} - \min_{\text{acyclic}}}. \quad (5f)$$

For the data based on the moving sequences, the prior distribution consists of two continuous as well as one discrete uniform distribution. The parameter set is composed by the interval limits $[c_{\text{k-means},0}, c_{\text{k-means},k-1}]$ of the discrete uniform distribution over the identities and the altogether four intervals for the two bases $\mathbf{b}_{\min}$ and $\mathbf{b}_{\max}$. The composition of a sample $\mathbf{z}$ from this defined prior distribution can be formally described by

$$z_1 \sim U(s_{\text{x, min}}, s_{\text{x, max}}), \quad (6a)$$

$$z_2 \sim U(s_{\text{y, min}}, s_{\text{y, max}}), \quad (6b)$$

$$z_3 \sim D(\boldsymbol{c}_{\text{k-means}}) \quad (6c)$$

$$\text{with} \quad (\boldsymbol{s}_{\text{x}}, \boldsymbol{s}_{\text{y}})^T = h \cdot (\mathbf{b}_{\max} - \mathbf{b}_{\min}) + \mathbf{b}_{\min}, \quad (6d)$$

$$h = \frac{z_3 - c_{\text{k-means},0}}{c_{\text{k-means},k-1} - c_{\text{k-means},0}}. \quad (6e)$$

Note that a rotation to align the distributions with the coordinate axes has to be learned. Fortunately, this rotation is a by-product of the Independent Component Analysis (ICA) step of the following fitting procedure. The corresponding inverse is calculated by default in the used implementation of ICA (Pedregosa et al., 2011) and is justifiable in terms of computational costs when the latent space is low-dimensional.

We fit these general parameterized prior distributions to embedded data by estimating the individual parameters. The fitting procedure developed and applied for this purpose consists of four steps:

1. Embedding the data,
2. finding rotation and inverse,
3. identifying cyclic/acyclic and discrete/continuous dimensions,
4. estimating parameters.

The embedded data is first rotated to align the distributions with the coordinate axes by ICA. Note that due to the SFA constraints the embedding does not need to be whitened beforehand.

To determine continuous and categorical dimensions, we first build a 100-bin histogram for each axis. Afterwards, the axis is either classified as discrete or continuous depending on the variance over the frequency per bin. Using this heuristic, we are able to reliably distinguish between continuous and categorical dimensions by a hard threshold. Cyclicity is determined by thresholding the variance for each axis over the distances from the respective axis to all data points, with an acyclic variable being coded along the axis with the smallest variance. Thus, each axis is matched with one marginal distribution.

Subsequently, the parameters of each marginal can be estimated directly from the rotated embedding. The interval limits of continuous uniform distributions are given by the minimum and maximum values of the respective dimension. For each categorical dimension, we perform k-means clustering to identify the corresponding discrete values over which a uniform distribution is defined. We set the mean values of the distances to the acyclic axis of the points at the ends of the conical frustum as the radii of the ellipses.

To sample from the thus fitted prior distributions, samples are drawn from each marginal and then back-transformed by the inverse of the rotation matrix previously determined by ICA in order to align them with the original embedding.

Figure 7 visualizes the latent space with the two considered embedded datasets (orange) and samples taken from the defined and fitted prior distributions (blue). The samples show that the parameters have been well estimated and the fitted prior distributions accurately abstract the embedding of the datasets. To generate new image data, we use the decoder to decode the drawn latent samples. The resulting images shown in Figure 7 demonstrate that the samples from the prior distribution represent all variations and can be decoded meaningfully and accurately by the decoder.

In conclusion, we state that this procedure represents a practicable approach for the posterior definition and estimation of a prior distribution over latent factors in the context of the data considered in this work. By sampling from the defined prior distribution and decoding the obtained latent data point, the generation of a new image accurately matching the original input images is enabled.

This method is of course not limited to the data considered here, but can be applied to any data with corresponding continuous, categorical and cyclic or acyclic underlying variables and latent factors. Assuming a sufficiently powerful extraction, the characteristic distributions defined here should be applicable.

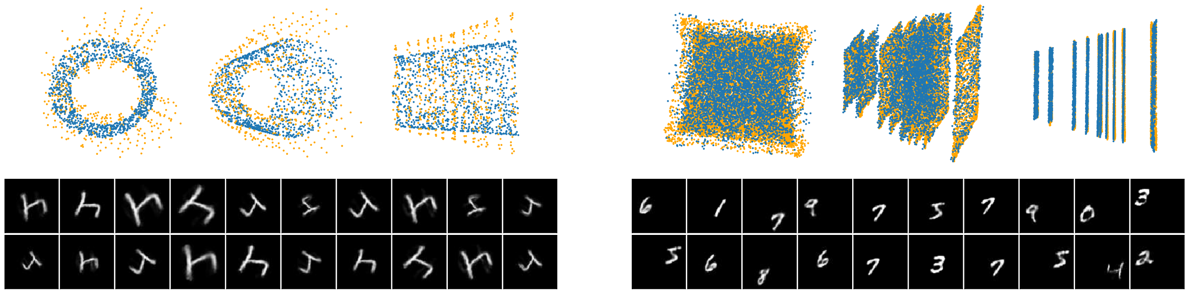

(a) (b)

Figure 7: Three views of the embedding (orange) and latent samples drawn from the fitted prior distribution (blue) as well as exemplary generated images based on these latent samples of data with variation in rotation and scaling (a) and variation in position and identity (b).

3.5.2 Prediction of Latent Samples for Sequence Generation

In this last section, we present an approach for generating not only single images but whole image sequences. We extend the Encoder-Decoder model by a predictor over the latent factors. The predictor is embedded between the encoder and the decoder and receives ten successive features as an input sequence. This input is passed through two layers consisting of 64 and 32 Long Short Term Memory (LSTM) units. After applying the ReLU activation function, the output is reshaped into a sequence of ten features which are finally fed into the decoder to generate an image sequence.

To train the predictor, we optimize the parameters with respect to the mean absolute error between the predicted sequences and the target sequences using the stochastic gradient-based RMSprop optimization method (Tieleman and Hinton, 2012).

We have analyzed the resulting Encoder-Predictor-Decoder model on different datasets in the context of both static and moving sequences. In the following, the results obtained by training on data with variation in position and within a set of ten identities are presented. For this purpose, we embed the predictor into the What-Where Encoder-Decoder model. The sequences of the dataset consist of 20 images each, where the first half is used as the input sequence and the second half as the target sequence.

Considering the validation and test error of the predictor, it can be summarized that based on the input sequences, the predictor accurately predicts the ten following features. The output images computed by the decoder reconstruct the position and identity in the individual images qualitatively well and the attributes change smoothly and conclusively in the course of the sequence. The predicted image sequence thus corresponds precisely to the respective ground truth and continue the input sequence in a reasonable and conclusive way as shown in Figure 8. Qualitatively similar results could also be achieved on datasets with other varying attributes.

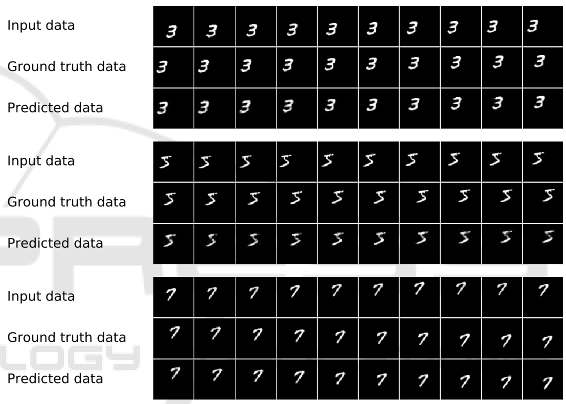

Figure 8: Image sequences generated by the decoder of the What-Where Encoder-Decoder model based on predicted samples for data with variation in position and identity.

We summarize that by extending the Encoder-Decoder model by a predictor for predicting latent features, precise and meaningful image sequences can be generated. These results therefore support the hypothesis that the features extracted by SFA are suitable as a basis not only for the generation of single images as shown in Section 3.5.1, but also for the generation of sequences of images.

Note that the prediction of image sequences based on predicted latent feature values offers two elementary advantages compared to a prediction directly on the input data. First, the predictor only has to learn and predict the abstract underlying dynamics in the low-dimensional latent space. Second, the quality of the generated images always remains the same and no distortions or blurring can occur as in some other approaches due to the collapse of complex LSTMs.

4 DISCUSSION

In this paper, we explored SFA for the extraction of generative latent factors. We developed different models and evaluated them on a variety of datasets with different data-generating attributes. In this evaluation, we found that the extraction principle of slowness is in general not contrary to reconstructability from low-dimensional representations, while providing the corresponding space with additional properties beneficial for generative tasks as has been demonstrated in Section 3.4. However, while slow features live in a structured, continuous and complete space, the specific nature of the extracted features is governed by the types of latent variables used in data generation and can negatively impact the overall quality of the reconstruction in specific cases.

One of these cases is identified as the mixing of continuous with categorical latent variables and is subsequently addressed in Section 3.4.3 by development of the What-Where Encode-Decoder model using two qualitatively different extraction paths.

Finally, to complete a possible generative model based on SFA, a prior distribution had to be constructed. As construction of suitable prior distributions is in general a hard problem, the chosen approach leveraged known structural properties of SFA-extracted features and was successfully applied for the case of single samples of a synthetic dataset when using a low-dimensional feature space in Section 3.5.1. A possible ansatz to also generate sequences was discussed in Section 3.5.2.

Future Directions. We see potential in continued investigation of SFA representations as foundation for generative models, as it also has been shown to extract useful representations even in the case of high-dimensional data. One limitation here might lie in the use of very low-dimensional latent spaces: While effective prior distributions can be constructed, not all interesting latent factors might be captured. Therefore, the authors regard the possible generalization of the identified construction principles to higher dimensions as the most promising research direction at this point.

REFERENCES

Böhmer, W., Grünewälder, S., Nickisch, H., and Obermayer, K. (2011). Regularized sparse kernel slow feature analysis. In Gunopulos, D., Hofmann, T., Malerba, D., and Vazirgiannis, M., editors, *Machine Learning and Knowledge Discovery in Databases*, pages 235–248, Berlin, Heidelberg. Springer Berlin Heidelberg.

Denton, E. and Fergus, R. (2018). Stochastic video generation with a learned prior. In Dy, J. and Krause, A., editors, *Proceedings of the 35th International Conference on Machine Learning*, volume 80 of *Proceedings of Machine Learning Research*, pages 1174–1183, Stockholmsmässan, Stockholm Sweden. PMLR.

Dozat, T. (2015). Incorporating nesterov momentum into adam. http://cs229.stanford.edu/proj2015/054_report.pdf.

Escalante-B, A. N. and Wiskott, L. (2020). Improved graph-based sfa: Information preservation complements the slowness principle. *Machine Learning*, 109(5):999–1037.

Franzius, M., Sprekeler, H., and Wiskott, L. (2007). Slowness and sparseness lead to place, head-direction, and spatial-view cells. *PLoS Computational Biology*, 3(8):1–18.

Franzius, M., Wilbert, N., and Wiskott, L. (2011). Invariant object recognition and pose estimation with slow feature analysis. *Neural Computation*, 23(9):2289–2323.

Goodfellow, I., Bengio, Y., and Courville, A. (2016). *Deep Learning*. MIT Press. http://www.deeplearningbook.org.

Goodfellow, I., Pouget-Abadie, J., Mirza, M., Xu, B., Warde-Farley, D., Ozair, S., Courville, A., and Bengio, Y. (2014). Generative adversarial nets. In Ghahramani, Z., Welling, M., Cortes, C., Lawrence, N. D., and Weinberger, K. Q., editors, *Advances in Neural Information Processing Systems 27*, pages 2672–2680. Curran Associates, Inc.

Hafner, D., Lillicrap, T., Ba, J., and Norouzi, M. (2020). Dream to control: Learning behaviors by latent imagination. In *International Conference on Learning Representations*.

Karras, T., Aila, T., Laine, S., and Lehtinen, J. (2018). Progressive growing of GANs for improved quality, stability, and variation. In *International Conference on Learning Representations*.

Kingma, D. P. and Ba, J. (2014). Adam: A method for stochastic optimization. *arXiv preprint arXiv:1412.6980*.

Kingma, D. P., Salimans, T., Jozefowicz, R., Chen, X., Sutskever, I., and Welling, M. (2016). Improved variational inference with inverse autoregressive flow. In *Advances in neural information processing systems*, pages 4743–4751.

Kingma, D. P. and Welling, M. (2013). Auto-encoding variational bayes. *arXiv preprint arXiv:1312.6114*.

Kingma, D. P. and Welling, M. (2019). An introduction to variational autoencoders. *Foundations and Trends® in Machine Learning*, 12(4):307–392.

LeCun, Y., Cortes, C., and Burges, C. (2010). Mnist handwritten digit database. http://yann.lecun.com/exdb/mnist.

Mehri, S., Kumar, K., Gulrajani, I., Kumar, R., Jain, S., Sotelo, J., Courville, A., and Bengio, Y. (2016). Samplernn: An unconditional end-to-end neural audio generation model. *arXiv preprint arXiv:1612.07837*.

Pedregosa, F., Varoquaux, G., Gramfort, A., Michel, V., Thirion, B., Grisel, O., Blondel, M., Prettenhofer, P., Weiss, R., Dubourg, V., Vanderplas, J., Passos, A., Cournapeau, D., Brucher, M., Perrot, M., and Duchesnay, E. (2011). Scikit-learn: Machine learning in Python. *Journal of Machine Learning Research*, 12:2825–2830.

Schüler, M., Hlynsson, H. D., and Wiskott, L. (2019). Gradient-based training of slow feature analysis by differentiable approximate whitening. In Lee, W. S. and Suzuki, T., editors, *Proceedings of The Eleventh Asian Conference on Machine Learning*, volume 101 of *Proceedings of Machine Learning Research*, pages 316–331, Nagoya, Japan. PMLR.

Srivastava, N., Mansimov, E., and Salakhudinov, R. (2015). Unsupervised learning of video representations using lstms. In *International conference on machine learning*, pages 843–852.

Sutton, R. S. and Barto, A. G. (2018). *Reinforcement learning: An introduction*. MIT press.

Tieleman, T. (2013). The affnist dataset. www.cs.toronto.edu/~tijmen/affNIST/.org.

Tieleman, T. and Hinton, G. (2012). Lecture 6.5-rmsprop: Divide the gradient by a running average of its recent magnitude. *COURSERA: Neural networks for machine learning*, 4(2):26–31.

Tulyakov, S., Liu, M.-Y., Yang, X., and Kautz, J. (2018). Mocogan: Decomposing motion and content for video generation. In *Proceedings of the IEEE conference on computer vision and pattern recognition*, pages 1526–1535.

Turner, R. and Sahani, M. (2007). A maximum-likelihood interpretation for slow feature analysis. *Neural Computation*, 19(4):1022–1038.

Van den Oord, A., Dieleman, S., Zen, H., Simonyan, K., Vinyals, O., Graves, A., Kalchbrenner, N., Senior, A., and Kavukcuoglu, K. (2016a). Wavenet: A generative model for raw audio. *arXiv preprint arXiv:1609.03499*.

Van den Oord, A., Kalchbrenner, N., Espeholt, L., Vinyals, O., Graves, A., et al. (2016b). Conditional image generation with pixelcnn decoders. In *Advances in neural information processing systems*, pages 4790–4798.

Wiskott, L. and Sejnowski, T. (2002). Slow feature analysis: Unsupervised learning of invariances. *Neural Computation*, 14(4):715–770.

Yarats, D., Zhang, A., Kostrikov, I., Amos, B., Pineau, J., and Fergus, R. (2019). Improving sample efficiency in model-free reinforcement learning from images. *arXiv preprint arXiv:1910.01741*.

APPENDIX

A Architectures and Code

Further details on the models, datasets and experiments can be found at https://github.com/m-menne/slow-generative-features.

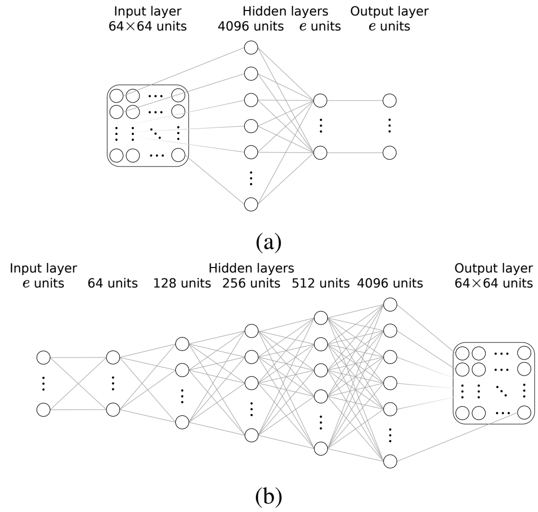

Figure 9: Architecture of the encoder (a) and decoder (b) network used in the different models.

B Influence of the Weighting Factor α

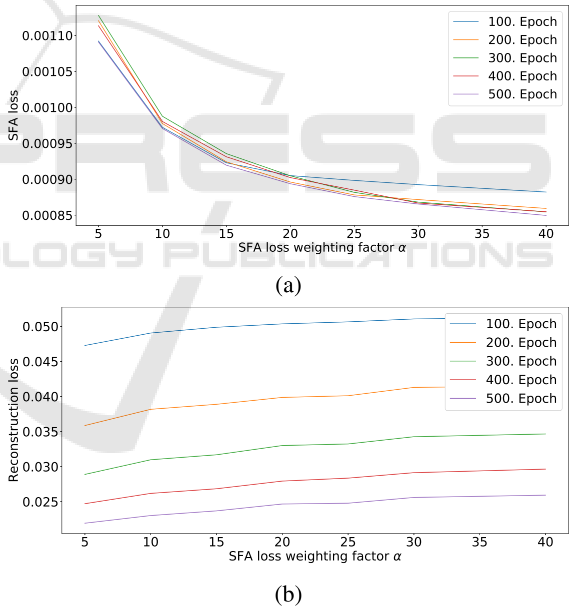

Figure 10: SFA loss (a) and reconstruction loss (b) in relation to the SFA weighting factor α after training for 100, 200, 300, 400 and 500 epochs.